The Sky Is Not Falling – Mechanical Damage Can Be Assessed Appropriately

Arnav Rana[1], Sanjay Tiku[1], Ali Roostaei[1], Behrouz Shiari[1], Vlado Semiga[1], Aaron Dinovitzer[2], Munendra Tomar[3], Yohann Miglis[4], Mark Piazza[5]

[1]BMT Canada, [2]ADIM Consulting, [3]TC Energy, [4]Kinder Morgan, [5]American Petroleum Institute

Organized by

CLARION
TECHNICAL CONFERENCES

https://doi.org/10.52202/078572-0045

https://doi.org/10.52202/078572-0045

Abstract

Dents or mechanical damage in buried pipelines can occur due to a number of potential causes; the pipe resting on rock, third party machinery strike, and rock strikes during backfilling, amongst others. The long-term integrity of a dented pipeline segment is a complex function of a variety of parameters including but not limited to pipe size, indentation depth, dent or indenter shape, indenter support, and pressure history at and following indentation. Operational experience and regulatory oversight have identified mechanical damage as a threat to pipeline integrity. As a response, industry has sponsored mechanical damage research (i.e., PRCI, US DOT PHMSA, CEPA, and others) and industry led by the American Petroleum Institute (API) developed a Recommended Practice (RP) for managing pipeline mechanical damage (API RP 1183). The first edition of API RP 1183 was assembled and published in 2020 by drawing together industry experience and engineering tools available at the time recognizing that improvements would be made. With use, opportunities for improvement in API RP 1183 have been identified and thus a second edition of the RP is being developed at this time.

The following paper is prepared to discuss the opportunity for improvement (OFI) observations that have been offered in the open literature related to some of the tools and techniques presented in API RP 1183. The observations are related primarily to the RP restraint condition, indentation strain, and fatigue life screening and analysis tools. The paper will address a range of OFI's, including but not limited to:

- the relative level of conservatism associated with the fatigue life screening tools and which has resulted in modifications to both the RP and the screening tool;
- misinterpretations or misapplications of the RP which have provided opportunities to improve how the tools and processes are communicated in the RP;
- engineering tools that are embedded in the state of engineering practice across industry standards that would require changes beyond the RP if adopted; and
- demonstrating engineering tool weaknesses that consider mechanical damage scenarios that are either unmeasurable using existing inspection technologies or are not considered likely to occur but provide opportunities to improve on the limits of application of the engineering tools presented in the RP

The objective of this paper is to provide engineering or science-based answers to the questions raised related to API RP 1183 mechanical damage management procedures and demonstrate that while there are opportunities for improvement, the engineering tools presented in API RP 1183 provide a sound basis for mechanical damage management in pipelines.

Introduction

Over the past decade significant work has been performed to extend our understanding of mechanical damage integrity management. Multiple research projects funded by PRCI, CEPA and US DOT have been undertaken in this regard. Extensive dent fatigue full-scale experimental (PRCI/DOT MD 4-2 [1], PRCI/DOT 4-11 [2], PRCI 4-14 [3], PRCI 4-15 [4]) and finite element

https://doi.org/10.52202/078572-0045

numerical modelling (PRCI MD 4-9 [5], PRCI MD 2-4 [6]) studies were conducted as part of these projects. In total, 127 full-scale tests and more than 1,000,000 finite element simulations have been conducted in these projects. Based on this comprehensive data, multiple dent fatigue life screening (Level 0, 0.5, 0.75) [7] [8] [9] [10] and assessment (Level 2 [5] [6]) engineering models have been developed to predict conservative fatigue life estimates, without resorting to involved finite element analyses. Some of these models have also been incorporated into the first edition of API RP 1183 [11]. Extensive validation of these developed models has also been conducted through comparisons against full-scale test data and in-field inspection data (PRCI MD 2-5 [12] [13]). Work has also been conducted to quantify the effect of in-line inspection measurement variability in model predictions (PRCI/DOT MD 5-2 [14] and NDE 4-18 [15] [16]). In addition to the dent fatigue research, taking advantage of the extensive experimental and FE modelling data, work was also carried out in MD 5-2 to modify and improve the ASME B31.8 Appendix R strain formulation which is an important tool to predict cracking induced during indentation [14].

In recent publications [17] [18] [19] [20] [21] some concerns have been raised regarding the aforementioned dent fatigue life and strain formulations. Some of the issues raised in these publications dealt with the accuracy of the engineering models. However, the domain of the investigations have largely been either outside the scope of these models or presently cannot be reliably measured by ILI tools. Most of the engineering tools presented in the RP had been developed using regression analysis on large datasets and are not mechanistic models. The domain of fitting of these models covered a wide range of parameters but were limited to more practical considerations, with ILI measurability being one of them. Testing such engineering models across a wide variety of scenarios is an important exercise in developing a better understanding but considerations regarding the applicability of these models should also be taken into account. The objective of this paper is to address the concerns raised and inform the readers about the considerable work that has been carried out to validate these engineering tools since the publication of API RP 1183 1st edition. This paper has been divided into two main sections, the first section addresses issues raised related to dent fatigue life assessment and the second section deals with issues raised regarding dent strain assessment.

Dent fatigue life assessment approaches

The Level 2 assessment approach, developed as part of the PRCI project MD 4-9 [5] and incorporated in the first edition of API RP 1183 [11], is a regression-based model which predicts the fatigue life of single peak dents as a function of dent shape and pressure-time history. The dent shape is represented by shape factors which are functions of characteristic lengths and areas of the axial and transverse profiles through the dent apex. The Level 2 assessment approach also employs a “restraint parameter” which can be used to distinguish between restrained and unrestrained dents, which behave differently. Updates/improvements to this approach have been proposed in PRCI projects MD 2-4 [6] and MD 5-03 [6]. In Ref [19], the specific issues raised were regarding the capability of the models to predict axial fatigue cracks seen in shallow restrained dents and with regards to element size used

https://doi.org/10.52202/078572-0045

in FE models used to develop the Level 2 assessment engineering tool. In Ref [20] [21], issues were raised regarding the correct implementation of the Level 2 approach, where improper use of both restrained and unrestrained dent fatigue life formulations for a single dent lead to erroneous life predictions. This issue has been addressed in other publications [10] [13].

The following section addresses these issues and provides a summary of the significant amount of validation work [6] [12] [13] carried out to support the Level 2 assessment model.

Shallow Restrained Dents

In multiple PRCI/CEPA projects, through both full-scale testing [1] [2] [3] and FE modelling [5] [7], the difference in behaviour between shallow and deep restrained dents has been extensively documented. In the full-scale tests it was observed that shallow restrained dents exhibited different fatigue behaviour compared to deeper dents. The difference manifested in the form of the location and orientation of fatigue cracking. Shallow restrained dents exhibited axial ID fatigue cracks at the dent peak while deep restrained dents exhibited circumferential ID cracks at the dent shoulders (**Figure 1**a). This effect has also been observed in dent FE modelling through the location and orientation of fatigue crack driving critical stress ranges (**Figure 1**b and **Figure 1**c) [5] [7]. Based on these experimental and numerical behaviours, different formulations were developed for shallow and deep restrained dents [5] [7] [9]. This illustrates that the FE modelling and the regression models developed in the PRCI/CEPA projects can replicate the mechanisms driving the transitions in behaviour observed in **Figure 1**. The ability to consider this change in behaviour of restrained dents is unique in the PRCI/CEPA models providing better predictive capabilities than other non-FEA based empirical models.

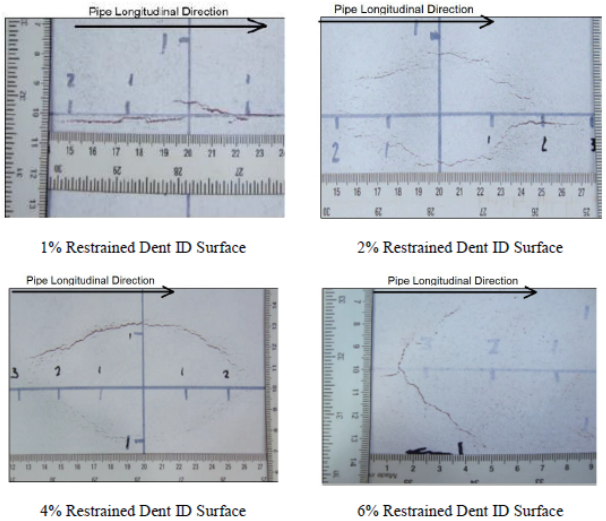

(a)

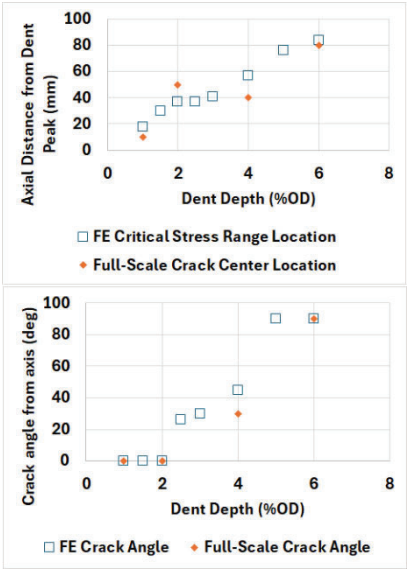

(b)

https://doi.org/10.52202/078572-0045

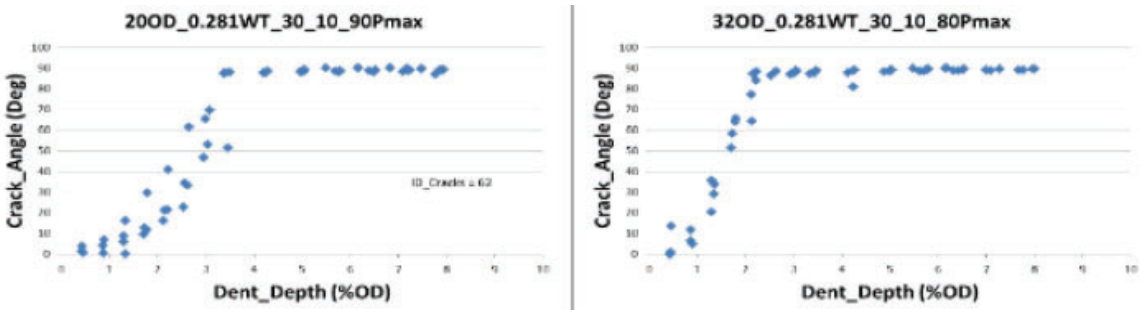

(c)

Figure 1. Transition of axial to circumferential cracking with increased dent depth in restrained dent (Test 25, 31, 32, 33) [5] [2] [3] (a) full-scale test ID photos (b) comparison of FE and full-scale critical stress range/crack center location and orientation (c) Transition of crack angle with dent depth in for 20" and 32" OD FE data

In Ref [19], Leis et al. have asserted that the unloading and flexure of the dent apex during pressure cycling in shallow restrained dents is responsible for the axial cracking, as opposed to circumferential cracking seen in deep restrained dents. It has also been stated in the paper, that a key assumption employed in the PRCI/CEPA projects was that for restrained dents the indenter immobilizes the dent apex, which would imply that the PRCI/CEPA models would be unable to account for the presence of axial fatigue cracks seen in shallow restrained dents. As has been demonstrated above, this is incorrect and the FE models developed as part of the PRCI/CEPA projects do accurately simulate the transition of crack orientation from axial to circumferential and from dent peak to dent shoulder, with increased depth in restrained dents.

Mesh refinement

The FE models employed in the PRCI/CEPA projects to develop the dent fatigue life screening and assessment engineering tools, use quadratic shell elements and an elastic-plastic kinematic hardening material model. More than a million FE cases have been simulated in the PRCI/CEPA projects that encompass a wide range of pipe geometries (4.5" to 42"OD), dent shapes (4" to 48" diameter, spherical/spheroidal/cylindrical indenters), dent depths (0.3% to 10%OD) and pressure conditions (e.g., pressure ranges - 10% to 70%PSMYS) [5] [6] [7] [8]. The FE model has been validated against 127 full-scale test data [1] [2] [3] [4], of which 20% of the dents had been removed from service and used in full-scale testing (MD 4-15). The full-scale tests consisted of a wide range of pipe geometries (10.75" to 40" OD), dent shapes, dent depths (0.3% to 11%OD) and pressure conditions (e.g., pressure ranges - 30% to 70% PSMYS). These field dents were instrumented with strain gauges and pressure cycled in the laboratory. The strain gauges were placed at different locations within the dent region including dent peak and dent shoulder. Numerical simulations of these dents were also carried out and the FE predictions were compared with experimental data. The final FE dent profiles and the pipe specimen laser scan profiles were compared to arrive at a matching shape. The strain range predictions from FE were compared against the experimental results which showed good agreement (**Figure 2**). Since, the primary focus of these tests was fatigue, the FE and experimental strain ranges were compared.

https://doi.org/10.52202/078572-0045

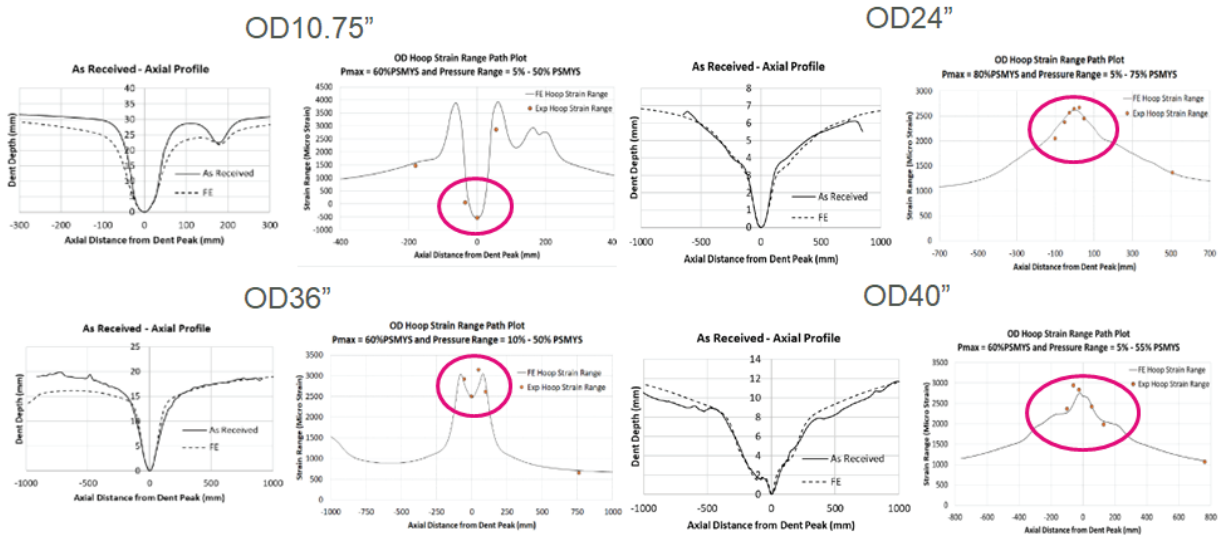

Figure 2. Examples of profile matching and comparison of FE and experimental of dent strain ranges

In Ref [17], the EPRG and API 579 recommendations regarding "kinked" dents (bending strain > 10% or dent radius of curvature < 5*WT) have been mentioned, along with the recommendation that shell elements not be used for modelling kinked dents. There were four dents in the MD 4-15 project that met the kinked dent requirement. Good agreement between FE and experimental values were also observed for these dents (**Figure 3**). The data provided in **Figure 2** and **Figure 3**, demonstrate that the FE modelling achieved good agreement with regards to dent shape as well as dent strain range. This level of agreement demonstrates a solid basis for the PRCI/CEPA models to predict dent fatigue life.

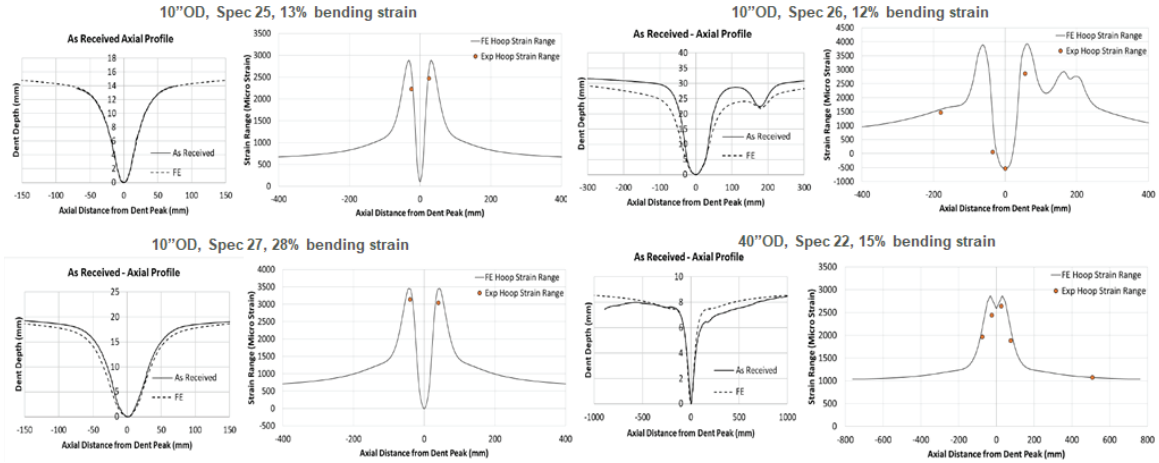

Figure 3. Examples of profile matching and comparison of FE and experimental of dent strain ranges for dents that meet the 'kink' criterion

https://doi.org/10.52202/078572-0045

In Ref [19], Leis et al. have presented a mesh sensitivity study which implied that the mesh sizes employed in the FE models used in PRCI/CEPA projects may not be adequate. The accuracy of the FE results across multiple mesh sizes were compared using equivalent plastic strain values at indentation. The focus of the discussion in this section is with regards to the accuracy of the FE modelling implemented in PRCI/CEPA projects for cyclic fatigue scenarios and not at indentation. The accuracy of the models with regards to cyclic loading has been clearly demonstrated above. The implication of the mesh sensitivity study provided in Ref [19] with regards to indentation strains will be discussed in detail in the strain section of this paper.

Overview of the work completed to validate and support the dent fatigue life assessment approaches

Since, the publication of the MD 4-9 report (2019) detailing the Level 2 fatigue assessment methodology, significant work has been completed to validate and support the analysis approach. In the PRCI MD 2-4 (2023) [6] and PRCI MD 2-5 (2024) [12] projects, extensive validation studies of the fatigue life assessment approaches have been conducted. Pertinent details from these projects have also been shared in an IPC 2024 paper [13]. The validation was performed against full-scale test data (127 dents), FE analysis of in-service dent data (1000 dents) and against in-ditch inspection data of field dents (>1000 dents). Arguably, more validation has been completed for the PRCI/CEPA dent fatigue life assessment approaches than any other published dent fatigue life approaches. In addition to validation of the fatigue life assessment approaches, work has also been completed to support their implementation. Significant inroads have been made in understanding the ILI measurement variability with regards to dent shapes and its impact on dent fatigue life predictions, through the PRCI/DOT NDE 4-18 project [15] [16] involving full scale ILI trials for various dent features. Nine ILI service providers participated in the trials where the various ILI systems were run multiple times (up to 10 times per ILI system) through pipe test strings which included more than 100 unique dent features. The collated measurement data allowed the quantification of the ILI measurement variability and its effect on dent fatigue life predictions. The following sections, present a brief summary of the projects mentioned above.

Finite element and experimental validation of Level 2 approach

In PRCI MD 2-4 [6] [13], the Level 2 assessment methodology was verified against in-service dent FE analysis results and full-scale test data. As part of the project, an update/improvement to the Level 2 approach was also developed (fitted on more than 1,000,000 FE scenarios). FE analysis data from 1000 single peak in-service dents from multiple pipeline operators were available. The in-service dents ranged from 0.3% to 8% OD in depth over a wide range of pipe geometries (8" - 42" OD). In addition, the experimental results from 127 full-scale dent fatigue test data [1] [2] [3] [4] were also used in the validation. The dent maximum stress ranges predicted from FEA for both the in-service and full-scale dents were compared against the predictions of the Level 2 approach (**Figure 4**a and **Figure 4**b). Good agreement was observed with approximately 70% and 90% of the data, within 10% and 20% scatter bands, respectively. The fatigue life predictions made using the Level 2 approaches

https://doi.org/10.52202/078572-0045

were compared to the full-scale dent experimental lives with 98% of the Level 2 predictions being conservative compared to experimental lives (**Figure 4**c).

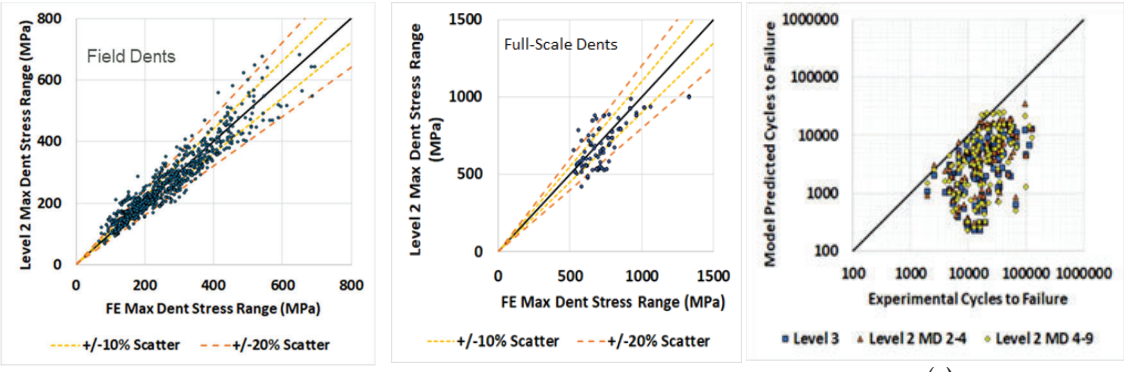

(a) (b) (c)

Figure 4. Unity plots of FE vs Level 2 dent stress ranges for (a) field dents and (b) full-scale test dents, with ±10% and ±20% scatter bands. (c) Comparison of Level 2 and Level 3 FE predicted dent fatigue life with experimental data

Validation against in-ditch inspection data of field dents

As part of the PRCI MD 2-5 project [12] [13], in-ditch field inspection data for 1021 single peak dents were provided by multiple pipeline operators. These dents were originally identified as part of the operators' integrity management programs and had been excavated. For each dent evaluated in the study, 3D ILI dent radii data was provided along with operating pressure time history data. In-ditch inspection data provided information regarding the presence of leaks, cracks, interacting features etc. The collated dataset consisted of highly varied dent shapes (dent depths ranging from 0.3% to 7%OD), pressure cycling severity (Spectrum severity indicator [SSI] [11] ranging from 20 to 7000; SSI is the number of 13 ksi/90 MPa stress cycles that cause the same amount of fatigue damage per year as the actual cyclic pressure history) and pipe geometries (10" to 48" OD) (**Figure 5**).

Field dig and ILI inspection data for 1021 single peak dents were included in the MD 2-5 dataset, of which 5 dents were reported as having developed leaks. In addition, surface cracks (but no leaks) were reported being present in 100 additional dents. The various fatigue life screening and assessment approaches were applied to the single peak dents (**Figure 6**). The fatigue life predicted using the various fatigue screening and assessment approaches represents the time to form a through wall crack resulting in a leak. In the validation analysis, a dent with remaining fatigue life prediction less than 1 year from the date the dent was inspected was considered to have failed (i.e. leaked). When the dent had a remaining fatigue life <40 years from the date of dent inspection, it was considered to have violated a conservative threshold based on an integrity management/inspection interval point of view.

- With both thresholds, the Level 2 assessment approach correctly identified all of the dents with reported leaks.
- Most of the dents (approximately 60%) with surface cracks (but no leak) were also conservatively identified by the Level 2 approach. For the dents with cracks (but no leaks)

https://doi.org/10.52202/078572-0045

that passed the Level 2 assessment, conservative fracture mechanics-based analyses of the dents, based on the NDE reported crack sizes, revealed that these dents had significant predicted remaining life until the surface cracks grew to a through thickness crack (>50 years for most cases).

- Most of the dents without cracks appropriately passed the Level 2 assessment.

The results of this study demonstrate that the Level 2 fatigue life assessment approach is sufficiently conservative to identify critical dents with leaks and cracks, while not unnecessarily penalizing benign dents (**Figure 7**). Since all of the dents included in the study were excavated based on the operators' internal integrity management programs, use of this assessment could have prevented remediation for 671 of 1021 dents, even if the conservative <40 years threshold for failure had been applied. These results demonstrate the significant advantages that the operators can gain by incorporating the Level 2 assessment approach into their integrity management programs.

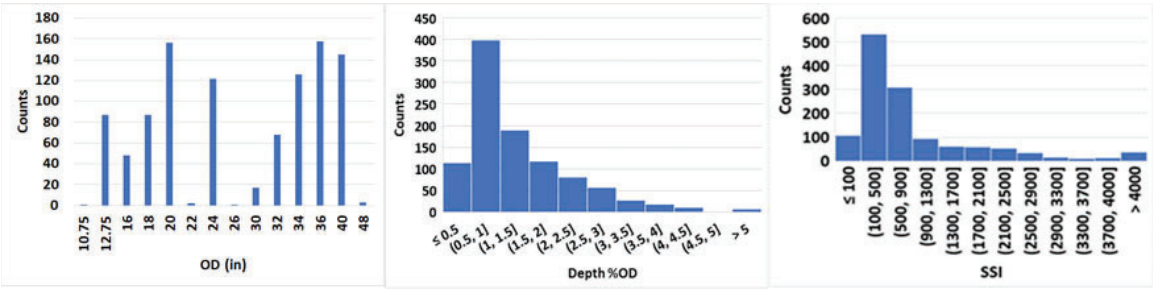

Figure 5. 1021 single peak dent statistics

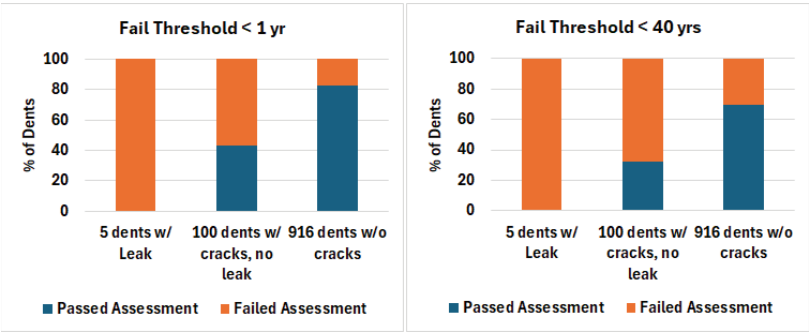

Figure 6. Charts showing pass/fail percentages of dents assessed using Level 2 approach

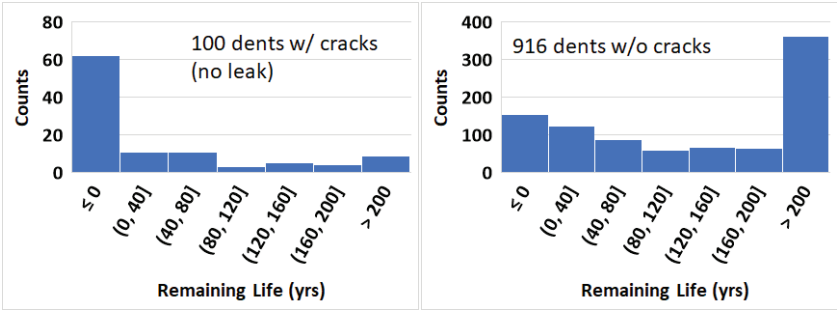

Figure 7. Remaining fatigue life estimates

https://doi.org/10.52202/078572-0045

As part of the MD 2-5 project, a validation study was also conducted for the restraint parameter [12] [13]. The parameter predicts the restraint condition of single peak dents based on the dent shape. The in-ditch inspection data of the dents with cracks was used to perform the validation study. Based on the dent restraint condition the fatigue crack location can be different. For unrestrained dents, cracks develop on the OD surface, close to the dent peak while for restrained dents cracks form on the ID surface and can be closer to the dent shoulders. The restraint condition predicted using the restraint parameter were compared against the crack location information provided in the in-ditch NDE data. Based on the comparison, 94% of the dents predicted to be unrestrained exhibited OD cracks where 70% of these cracks were within an inch of the dent peak. Of the dents predicted to be unrestrained, 50% of the dents were on the top-side and 50% of the dents were on the bottom side, illustrating that bottom-side dents can also be unrestrained. For the dents predicted to be restrained, 97% were on the bottom-side. Contrary to expectation, for the dents predicted to be restrained only 45% exhibited ID cracks. But, in the remaining 55% of dents which exhibited OD cracks, the cracks were significantly away from the dent peak (7"-21" away) and were reported to be interacting with either corrosion, gouges or welds. This indicates that these cracks may not have been formed due to an unrestrained dent fatigue mechanism. Therefore, ruling out the cracks which were likely formed due to environmental factors (e.g., stress corrosion cracking) and which were reported to be significantly away from the likely dent fatigue cracking locations, the restrained parameter predictions agreed well (87% of cases) with the field observations.

Quantification of the effect of ILI measurement variability on fatigue life predictions

In the NDE 4-18 project [15] [16], nine ILI service providers (ISP) ran their systems though pipe test strings which included more than 100 single peak dents which were fabricated on pipe segments removed from service. Each service provider was required to run their ILI tool at 5 different speeds, with repeat runs at each speed (for a total of up to 10 runs per ILI tool). In total each dent was measured up to 80 times considering all tool runs from all service providers. The service providers provided 3D ILI data for each dent, from each tool run. From the provided 3D data, the analysis of the dent sizing variation across multiple ILI tools and run speeds was performed. In **Figure 8** and **Figure 9**, the variation in the dent profile measurements is illustrated for a few dents. **Figure 8**, presents the variations across different service providers, at a fixed tool speed, while **Figure 9**, presents the variation in profiles for a single service provider, across multiple tool speeds. **Figure 10**, presents the variation in ILI measured dent depth, compared against reference laser scan measured depth (95% of data points within ±1% OD scatter band).

https://doi.org/10.52202/078572-0045

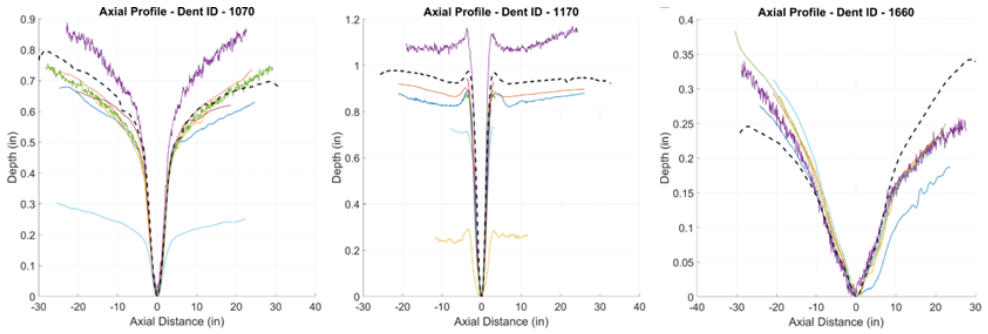

Figure 8. Variation in dent profile measurements across multiple ILI tools, at fixed tool speed

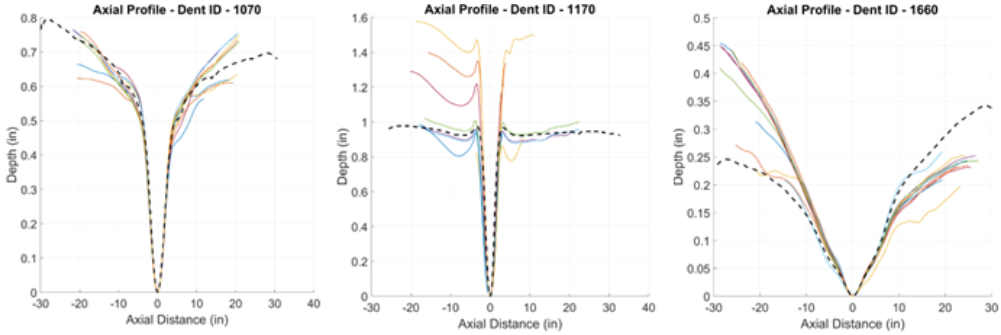

Figure 9. Variation in dent profile measurements across tool speeds, for a single ILI tool

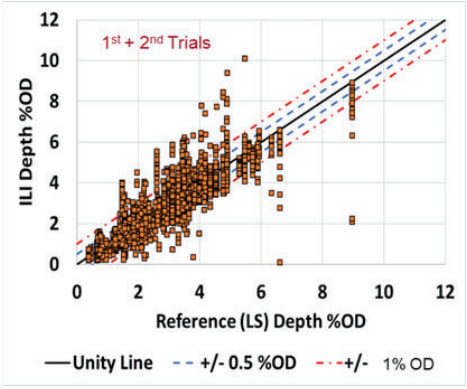

Figure 10. Unity plot comparing dent depth measurements from ILI and laser scan data

The accuracy of any fatigue life assessment approach which relies on ILI dent shape data is subject to the variation in the ILI measurements. This is true for relatively simple dent depth-based approaches like PRCI Level 0.75 [10] and EPRG Level 2 approach [22] to complex, elastic-plastic Level 3 FE analysis involving shape matching of FE profiles with ILI data. In NDE 4-18, the effect of ILI measurement variation on PRCI Level 2 fatigue life approach was quantified. The fatigue life estimates were evaluated for each ILI measurement of a dent (up to 80 measurements per dent) and the variation in the fatigue life predictions were evaluated for each dent. The variations were quantified by the coefficient of variation (COV, ratio of standard deviation to mean of distribution). For most dents the COV for fatigue life predictions was within 30% (**Figure 11**). The dent characteristic lengths and areas [5] [11], required for the Level 2 assessment, were extracted by both BMT and by most of the ILI service providers based on the 3D ILI dent data. **Figure 11**, presents the variation in the Level 2 fatigue life predictions for both the BMT extracted and the ILI service

https://doi.org/10.52202/078572-0045

provider extracted Level 2 parameters. It can be observed that there is good agreement between the two datasets which indicate that the Level 2 required parameters have been consistently extracted by multiple ILI service providers and that the shape parameter-based approach is reproducible by third parties. The two graphs in **Figure 11** are provided for ILI reported 3D dent shapes reported by two ILI service providers for the same dents. The 3D shapes of reported dents were different between these ILI service providers. However, when the reported 3D ILI dent data is used to calculate the characteristic lengths and depth parameters by the ILI service provider and BMT, very similar fatigue lives are predicted and the ILI service provider data on the graphs are close to the BMT calculated values.

Similar to the variation in fatigue life estimates, the variation in the calculated restraint parameter was also evaluated in the NDE 4-18 project **(Figure 12)**. For the majority of the dents, it was observed that the standard deviations of the calculated restraint parameter were less than 10. This finding motivated an update to the guidelines for using the restraint parameter, which attempts to account for the ILI measurement variation [10] [13].

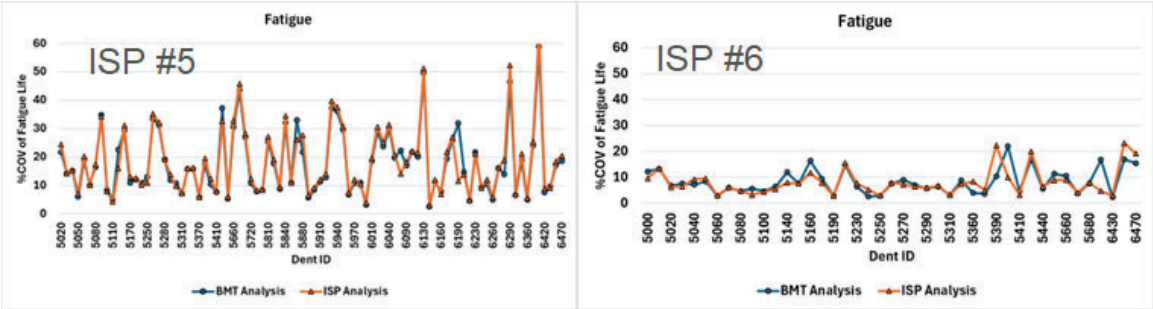

Figure 11. %COV of fatigue lives estimates across multiple dents for two ILI service providers

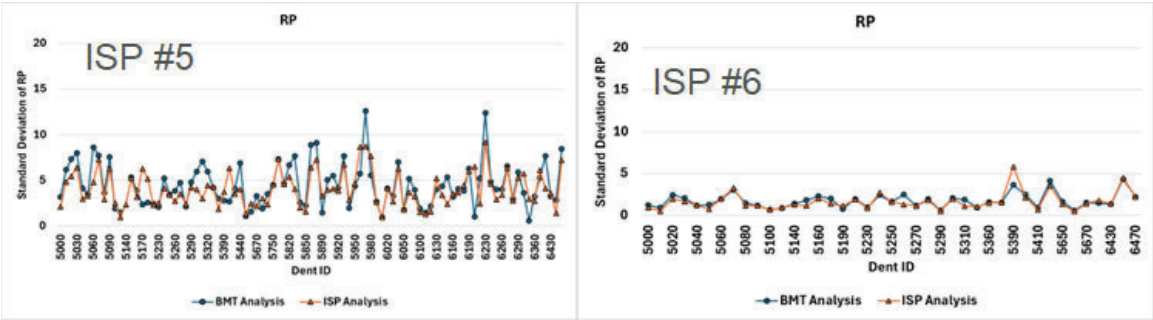

Figure 12. Standard deviation of restraint parameter estimates across multiple dents for two ILI service providers

As part of the MD 5-2 project [14] [23], a hypothetical Monte-Carlo study of the effect of dent measurement variation on fatigue life predictions was conducted. Approximately 900 field dent ILI profiles were varied based on various schemes to produce more than 1,000,000 variations of each dent shape. The variation schemes involved individual or collective variation (scaling) of the dent depth, length and width based on error samples extracted from normal distributions defined for a wide range of sizing tolerance values (10%, 15%, 20%). For each dent, fatigue lives were calculated for all shape variations within each scheme. The COV of calculated fatigue lives across all variation

https://doi.org/10.52202/078572-0045

schemes were less than 35%, which agrees well with the actual variation statistics evaluated in the NDE 4-18 project (**Figure 13**). This result suggests that ILI measurement variability, as measured in the ILI trails, does not excessively affect the fatigue life predictions of the assessment tools.

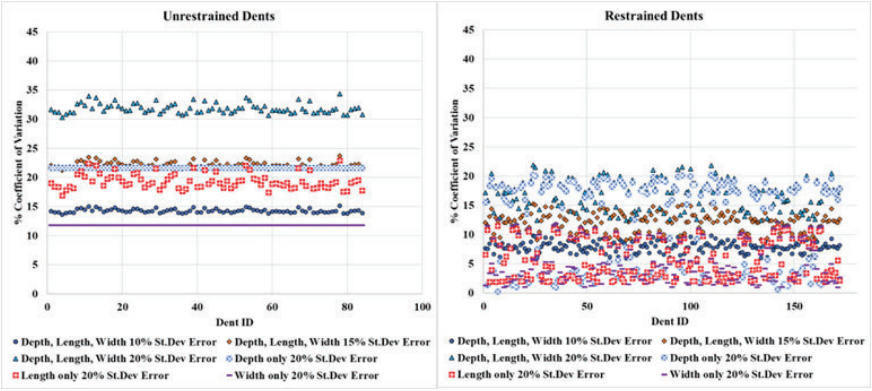

Figure 13. %COV of fatigue life from hypothetical Monte-Carlo dent shape variation study [14]

In addition to quantifying the effect of ILI measurement variation on dent fatigue life assessment, the effect of variation of ILI data on dent strain assessment was also studied in the MD 5-2 and NDE 4-18 projects. Dent strain was evaluated from the ILI dent peak curvatures using the ASME B31.8 Appendix R strain formulation [24]. COV of calculated dent strain from hypothetical (MD 5-2) and actual variation data (NDE 4-18, for all participating ILI caliper systems) have been provided in **Figure 14**. It can be observed that for most dents the COV of dent strain was within 60% in both studies. This result suggests that the dent strain calculations based on ILI dent peak curvatures can be more sensitive to ILI measurement variations than dent fatigue life estimates.

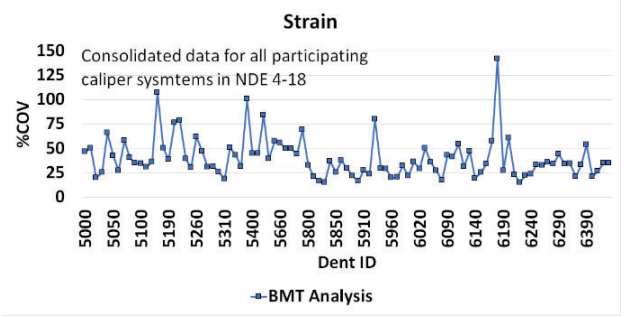

(a)

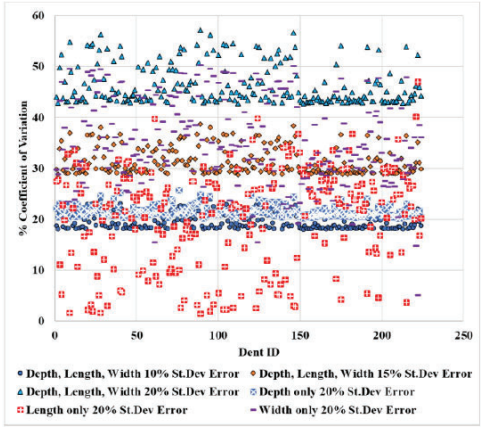

(b)

Figure 14. (a) %COV of dent strain for all participating ILI caliper systems in NDE 4-18 project (b) %COV of dent strain from hypothetical Monte-Carlo dent shape variation study

Other works completed to support/enhance fatigue life assessment approach

Multiple conservative screening approaches (Level 0 to 0.75) [7] [8] [9][1] [10] with fewer input requirements have been developed to complement the Level 2 assessment approach, using the same dent FE database (>1,000,000 cases) used to develop Level 2 assessment (**Figure 15**a). These provide

[1] Some of the CEPA project reports [7] [8] [9] may be accessible through CSA

https://doi.org/10.52202/078572-0045

lower-bound fatigue life predictions with minimal dent geometry or cyclic pressure input requirements. The level of conservatism decreases while the complexity of the input requirement increases with higher levels. In the MD 2-5 project, the screening approaches were also used for fatigue life estimation of 1021 single peak field dents and the fatigue life predictions were compared against in-ditch data. It can be observed in Figure 15b that these approaches provide conservative fatigue life estimates. As mentioned earlier, an update/improvement to the Level 2 approach was also developed in MD 2-4 project which was fitted using more than 1,000,000 FE cases and requires the same input parameters [6]. Unlike the original MD 4-9 approach, this approach predicts dent stress range via K_M which offers the flexibility of use of different S-N curves and can be applicable to fracture-mechanics based fatigue crack growth analyses.

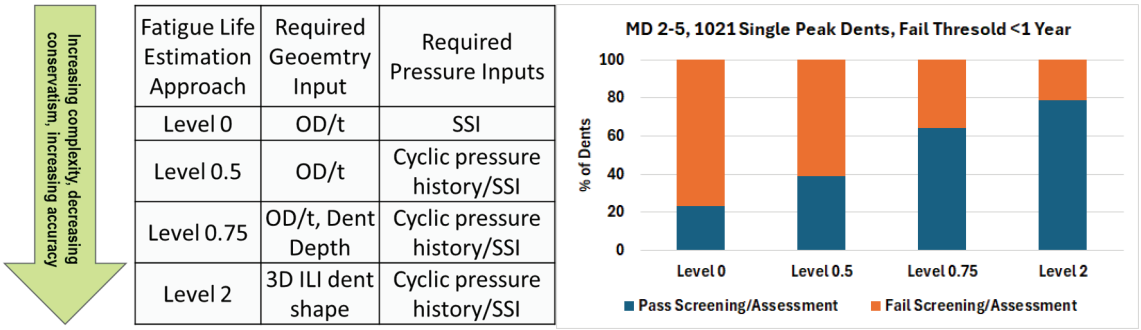

Fatigue Life Estimation Approach	Required Geoemtry Input	Required Pressure Inputs
Level 0	OD/t	SSI
Level 0.5	OD/t	Cyclic pressure history/SSI
Level 0.75	OD/t, Dent Depth	Cyclic pressure history/SSI
Level 2	3D ILI dent shape	Cyclic pressure history/SSI

(a) (b)

Figure 15. (a) List of dent fatigue life screening and assessment approaches (b) Charts showing pass/fail percentages of 1021 single peak field dents assessed using different screening and assessment approaches in the MD 2-5 project

In the PRCI MD 5-2 [14] [23], 5-03 [10] and 2-4 [6] [25] projects, safety factor quantification using full-scale test data, for various fatigue life screening and assessment approaches, have been developed. These developments can be implemented to achieve different factors of safety in fatigue life assessments as required by regulations or operator practices. In the PRCI 2-4 [6] [25] project, the dent fatigue weld interaction criteria have also been updated to reduce the excessive conservatism (i.e., use of a 10x life reduction) associated with the original criteria provided in MD 4-9 and API RP 1183. This development significantly reduces the excessive conservatism of the previous approach without compromising safety.

A conservative fracture mechanics-based approach has been developed to account for dent-crack and dent-metal loss (gouge) interactions with regards to fatigue [6] [10]. The maximum stress range predicted from the screening and assessment approaches can be conservatively implemented as a membrane stress range to be used in BS 7910 [26] or API 579 [22] Paris crack growth calculations to predict the life until a leak would occur. This approach was also validated against full-scale tests where notches were fabricated into dents and subjected to cyclic pressure loading (Figure 16a). Notches were fabricated at both the dent peak and the dent shoulders, depending on the location of the plain

https://doi.org/10.52202/078572-0045

dent critical stress range. Compared to experimental data, the screening and assessment approaches predicted conservative fatigue crack growth lives (Figure 16b).

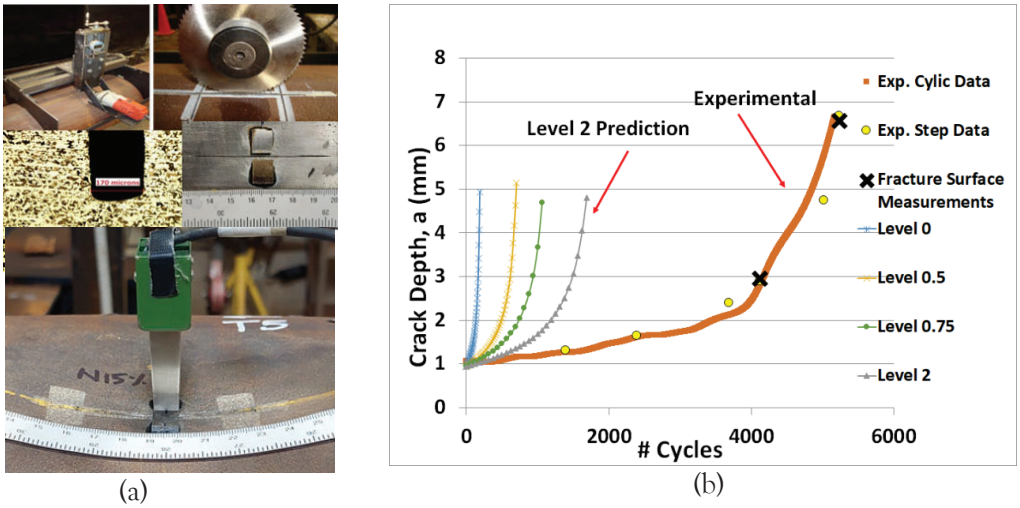

(a) (b)

Figure 16. (a) Full-scale dent machined notch (b) Comparison of predicted and experimental crack growth curve

Summary of fatigue life discussions

The concerns raised in Ref [19] regarding shallow restrained dents and FE model mesh accuracy were addressed in this section and the methods developed based on significant studies completed by PRCI and US DOT PHMSA were demonstrated to be appropriate for dent fatigue assessments based on:

- Comprehensive data validating the Level 2 fatigue life assessment and FE modelling approaches were provided from a wide range of sources – full-scale test data (127 dents), FE analysis of in-service dents (1000 dents), in-ditch inspection data of field dents (>1000 dents), etc. The models were shown to agree with the provided full-scale and field data.
- Discussions regarding the quantification of ILI dent measurement variability was covered. The variation data provides insight into the effect of ILI measurement variability on fatigue life and restraint parameter estimations. The ILI dent parameters were observed to be consistently extracted by the participating service providers.
- Discussions regarding other works completed to support and enhance the assessment approaches were also provided.
- It was demonstrated that the incorporation of the dent fatigue assessment tools into the integrity management programs will provide the operators with conservative fatigue life predictions without excessive calls for remediations.

Up to this point in the paper, discussions have been focused on dent fatigue life assessment. In the following sections the work completed with regards to dent strain estimation will be discussed.

Dent strain assessment approaches

https://doi.org/10.52202/078572-0045

In the PRCI/DOT MD 5-2 project the extensive FE dent database developed as part of multiple PRCI/CEPA projects [5] [6] was employed to study the widely used ASME B31.8 Appendix R (2018) [24] (included in API 1183) strain formulation. Based on a comparison of the ASME effective strains against FE strain results, modifications were proposed to improve the predictive accuracy of the ASME effective strain formulation. Additionally, a regression-based model was also developed to predict ASME effective strains at indentation for unrestrained dents. In some recent publications by Leis et al. [17] [18] [19], concerns regarding the ASME effective strain formulation and the modifications provided in MD 5-2 have been raised. In order to address the concerns raised, some background regarding the MD 5-2 work is provided in the following sections.

Background

The ASME formulation predicts an "effective" strain (ε_{eff}^{ASME}) as a function of the curvatures at the dent peak, the dent length and the dent depth, i.e., dent peak geometry. The ASME effective strain measure was devised as an analogue or approximation of the equivalent plastic strain (ε_{eq}^{p}). The equivalent plastic strain is used as a measure of ductile damage and denotes the history of plastic deformation [27]. It is a path-dependent function of plastic strain rate components and is always increasing if plastic flow occurs (Equation 1).

$$\varepsilon_{eq}^{p} = \int_0^t \sqrt{\frac{2}{3}\left(\dot{\varepsilon}_{11}^{p\ 2} + \dot{\varepsilon}_{22}^{p\ 2} + \dot{\varepsilon}_{33}^{p\ 2} + 2\dot{\varepsilon}_{12}^{p\ 2} + 2\dot{\varepsilon}_{13}^{p\ 2} + 2\dot{\varepsilon}_{23}^{p\ 2}\right)}\, dt \tag{1}$$

The equivalent plastic strain can only be evaluated incrementally using FEA and cannot be measured using just the dent geometry. The ASME effective strain measure is based only on the dent geometry and does not consider the deformation history. The ASME effective strain and equivalent plastic strain values for a dent can converge only if the deformation is under proportional loading [28], the elastic strain is very small compared to plastic strain and shear strain is negligible.

The focus in the MD 5-2 project was on ASME effective strain which is a geometric strain measure and not a measure of accumulated plastic deformation. Therefore, in the MD 5-2 project, the ASME effective strain was not compared to FE equivalent plastic strain but rather to FE "effective" strain (ε_{eff}^{FE}) which is also a geometric strain measure and a function of the total strain components.

$$\varepsilon_{eff}^{FE} = \sqrt{\frac{2}{3}\left(\varepsilon_{11}^{2} + \varepsilon_{22}^{2} + \varepsilon_{33}^{2} + 2\varepsilon_{12}^{2} + 2\varepsilon_{13}^{2} + 2\varepsilon_{23}^{2}\right)} \tag{2}$$

If the shear components are ignored and the strains are formulated in terms of bending and membrane components then Equation 2 can reduce to the ASME effective strain formulation. The goal of the study was to compare ASME effective strain against FE results, with regards to its ability to accurately measure the dent peak geometric strain at indentation. Therefore, comparison against FE effective strain rather than FE equivalent plastic strain is more appropriate as both are history-independent measures of dent geometry strains.

https://doi.org/10.52202/078572-0045

In the MD 5-2 project, the ε_{eff}^{ASME} values evaluated from the FE dent shapes were compared to ε_{eff}^{FE} values evaluated from the dent strain components extracted from the FE analysis. The comparison was carried out at the end of the indentation step as the primary focus was on dent formation strains. The FE database used for these comparisons consisted of approximately 4800 unique indentation cases for a range of pipe geometries (4" to 42"OD), dent shapes (4" to 48" spherical / spheroidal/ cylindrical indenters), dent depths (0.3% to 10%OD) and pressure conditions (e.g., indentation pressures – 20% to 90% PSMYS) [14]. For pipes with OD $\leq$ 12.75", mesh size of 2 mm was used in FE modelling, at the indenter contact region. For pipes with 12.75" $<$ OD $\leq$ 20", mesh size of 3 mm was used while the rest (OD$>$20") were modelled with 4 mm mesh size at the contact region.

The comparison of ASME effective strain and FE effective strain at indentation is shown in **Figure 17**a. For effective strain values $\leq$ 0.15 (i.e., 15%), good agreement was observed. The deviation at higher strains was considered to be due to the lack of proper membrane strain formulations in the ASME model. A modified ASME model was proposed which included an updated axial membrane strain and a circumferential membrane strain developed based on the framework of the axial membrane strain. Based on the FE results, references for dent depth and length required for accurate membrane strain calculations were also recommended. A set reference to calculate the dent depth and length is not provided in ASME B31.8 (2018). The modified ASME effective strain was in better agreement with the FE results (**Figure 17**b). The Blade Energy Partners effective strain [29] was also tested and was found to perform similarly to the modified ASME effective strain (**Figure 17**c and **Figure 17**d).

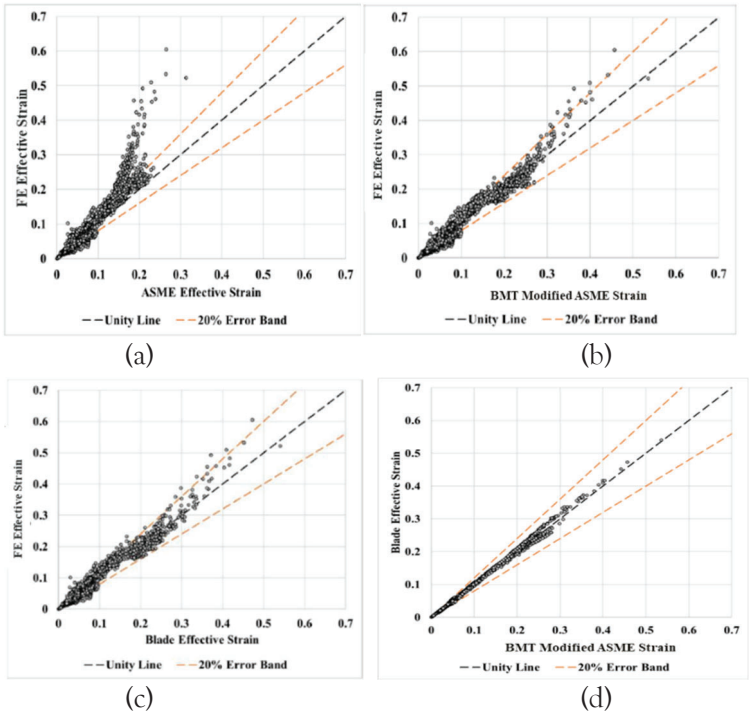

Figure 17. Unity plots comparing (a) ASME vs FE effective strain (b) modified ASME vs FE effective strain (c) Blade effective vs FE effective strain (d) modified ASME vs Blade effective strain

https://doi.org/10.52202/078572-0045

In addition to the updates to the ASME effective strain model, a simple regression model was developed to predict the ASME effective strains at the time of indentation for unrestrained dents. For unrestrained dents, dent peak strains can change significantly after indenter removal and pressure re-rounding. In contrast, the presence of the indenter prevents significant changes in the dent peak strains for the restrained dents, but small changes are observed [14] [23]. Therefore, a model that can estimate the ASME effective strain at indentation based on ASME effective strain measured by the ILI tool at pressure, for unrestrained dents was developed. Such a model was not developed for restrained dents since they exhibit similar strain values at indentation and under pressure. The model predicting indentation ASME effective strains for unrestrained dents was developed using 24,000 dent FE cases. The model takes on the following form [14] [23],

$$E_I = c_1 * E_P + c_2 * E_P^{|c_3|} \quad (3)$$

E_P is the dent peak ASME effective strain calculated based on the ILI measurements at pressure and E_I is the predicted dent peak ASME effective strain at indentation. The coefficients c_i are functions of pipe geometry and pressure. The range of parameter inputs used to fit Equation 3 have been provided in **Table 1**.

Table 1. Range of parameters used to fit Equation 3

Parameters	Values
OD/WT	24 to 128
Max pressure experienced by dent (%PSMYS)	20 to 90
Mean pressure (%PSMYS)	15 to 75
Indentation ASME effective strain	1% to 40%
ASME effective strain at pressure	0.01% to 30%

The goodness-of-fit of Equation 3 is presented in **Figure 18**. Overall, approximately 75% of the data points are within a 20% error band while approximately 95% are within 40% error band. Coefficients fitted to provide upper-bound predictions were also developed for greater conservatism. It is important to note that for the development of Equation 3, the E_I and E_P values were taken as the maximum of the ID and OD surface dent peak ASME effective strains at indentation and at pressure, respectively. Separate predictive equations for ID and OD surfaces were not developed. As can be observed in **Figure 18**, the model is able to relate strain values that are divided by complex plastic deformation histories with relatively simple equation and input requirements. Other authors have also developed similar models employing a similar approach and equation framework to achieve good results [30].

In the following sections the concerns raised by Leis et al. in Ref [17], [18] and [19] are addressed regarding the strain work presented in the MD 5-2 project. Primarily, the issues raised in the above cited references [17], [18] and [19] stem from incorrect comparisons of the MD 5-2 developments (which are only concerned with ASME effective strain) against FE equivalent plastic strains. The inherent differences in the two formulations (i.e., effective versus equivalent plastic strain) can result

https://doi.org/10.52202/078572-0045

in large errors, even without considering the scatter associated with the models included in the MD 5-2 project. Additionally, comparative analyses that were significantly outside the domain of fitting of the models developed in MD 5-2 (e.g., Equation 3), were implemented by the authors of these studies [17] [18] [19]. Application to such cases would inherently degrade the predictive accuracy of a regression model.

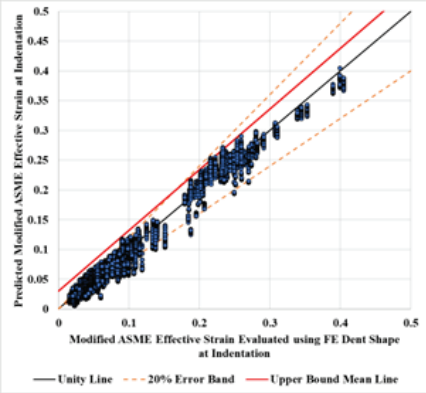

Figure 18. Unity line demonstrating the goodness-of-fit of Equation 3

FE strains used for comparisons with ASME effective strain values

In Figure 17a, a deviation can be observed between ASME and FE effective strains after 15% strain. This deviation was attributed to issues with the membrane strain formulation in the ASME effective strain and was corrected in the MD 5-2 project by modifying the ASME effective strain with improved membrane strain formulations (Figure 17b). The Blade effective strain [29] also exhibited similar performance compared to the modified ASME effective strain (Figure 17c and Figure 17d). In Ref [17], Section 3.2, Leis et al. have argued that the deviation in Figure 17a after 15% strain is due to improper comparison between ASME and FE strain values, with the implication that the conclusions drawn and improvements proposed in MD 5-2 are based on an incorrect analysis. They have argued that the discrepancies are due to the fact that:

- ASME effective strain is based on infinitesimal strain theory while the FE strains are based on large strain formulation,
- the ASME effective strains are being compared with FE equivalent plastic strains, and,
- the FE strains are based on logarithmic strains and not engineering strains.

The infinitesimal strain argument is not completely accurate. ASME [24], modified ASME [14] and Blade strains [29] are based on shell theory and include geometrically nonlinear membrane strain formulations which include second-order rotational components [31] [32]. Furthermore, in the MD 5-2 project the investigations were limited to indentation strains at the dent peak, which experiences minimal rotation due to indenter contact. This also renders the approximate strain formulation relatively accurate as large rotation, which is a major cause of deviation of small strain formulations from actual values, is not prevalent. In Ref [17], it has been incorrectly assumed that that FE equivalent plastic strains were used for comparison against ASME effective strains. As discussed

https://doi.org/10.52202/078572-0045

earlier, the geometry-based FE "effective" strains were employed, not the history-dependent equivalent plastic strains. It was also argued that since the FE strains were calculated using logarithmic strains, the FE values are higher than the ASME effective strains at values greater than 15%, with the implication that use of engineering-based FE strains would agree better with ASME effective strains. The FE effective strains were also calculated using engineering strain (Biot strain) [33] and are shown in (Figure 19). Even with FE effective strains based on engineering strain components, similar deviation is observed after 15% strain. Furthermore, almost all (99%) of the logarithmic FE strain components used to derive the FE effective strains were <20% [14], a threshold below which the differences are small between the logarithmic and engineering strain values. Therefore, the factors proposed in Ref [17], to the explain the deviation in Figure 17a, do not provide satisfactory reasons for the deviation. The application of modified ASME effective strain and the Blade effective strain approach (Figure 17 b and Figure 17c) do account for this deviation.

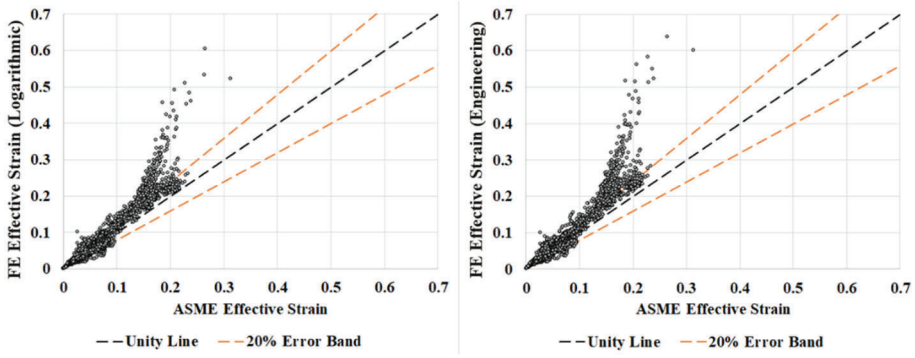

Figure 19. Comparing ASME with FE effective strains calculated using logarithmic and engineering strain components

Comparison of curvature-based ASME effective strains with equivalent plastic strains

As discussed earlier, the focus in the MD 5-2 project was on curvature-based ASME effective strains and a comparison of these values against geometry-based FE values. Within this scope, the formulations developed in the MD 5-2 project agreed well in comparison with FE results. In Ref [17], [18] and [19], Leis et al. have presented multiple comparisons of strains based on the ASME framework developed in MD 5-2, against FE strains. The majority of these comparisons have been against history-dependant equivalent plastic strain. These are inappropriate comparisons as there are inherent differences in ASME effective strain and equivalent plastic strain. The difference between these quantities can be demonstrated using the following example. FE analyses **(Table 2)** were performed to create an unrestrained dent on a 36"OD pipe and a restrained dent on a 24"OD pipe.

Table 2. Details regarding dent FE analyses

OD (in)	WT (in)	Grade	Indenter	Indentation Pressure (%PSMYS)	Indenter Travel (%OD)
36	0.375	X70	Spheroid (a=24", c=4")	0	7.5
24	0.281	X52	Spheroid (a=6", c=3")	0	1

https://doi.org/10.52202/078572-0045

The dent profiles at indentation and various pressures after indentation (20%, 50%, 80% PSMYS) are provided in **Figure 20**a and **Figure 20**b. The curvature-based ASME effective strains have been compared with equivalent plastic strains in **Figure 20**c and **Figure 20**d. For the unrestrained dent, a significant reduction in dent depth and peak sharpness (**Figure 20**a), resulting in a reduction in the ASME effective strains (**Figure 20**c), can be observed after indenter removal and pressure application. In contrast, the equivalent plastic strain continues to increase, due to accumulation of plastic damage, even though there is a reduction in dent depth and peak sharpness (**Figure 20**c). This clearly demonstrates the difference between geometry-based ASME effective strains and equivalent plastic strain. For the restrained dent the presence of the indenter prevents significant changes to the dent shape, but there is still significant difference between ASME effective strain and equivalent plastic strain (e.g., approximately 60% difference at indentation (**Figure 20**d)). This example demonstrates the extent to which the ASME and equivalent plastic strain values can differ. Therefore, the comparison of the ASME effective strains with equivalent plastic strain is inappropriate.

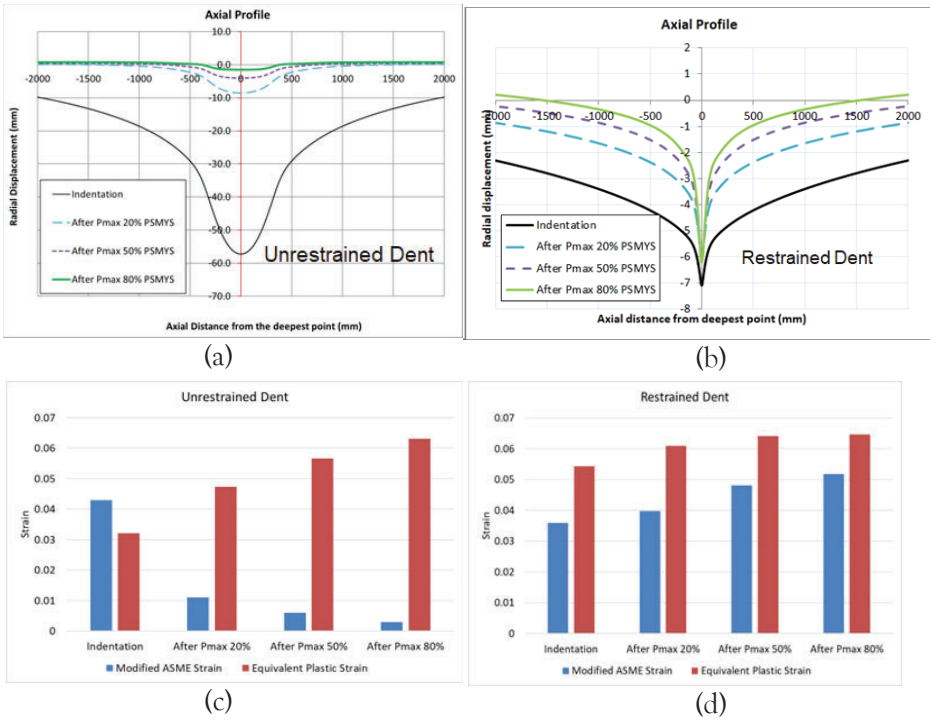

Figure 20. Variation of (a) unrestrained dent and (b) restrained dent axial profiles. Variation of (c) unrestrained dent and (d) restrained dent curvature and equivalent plastic strains

In Ref [17], [18] and [19], the majority of the comparisons have been inappropriately made between the curvature-based strains and equivalent plastic strains and large errors have been reported (≥±50%). When appropriate comparisons were made between geometry-based strains, the errors reported were within the scatter observed in the MD 5-2 project. Examples from Ref [17], Table 7, where appropriate comparisons had been made are presented in **Table 3**. In **Table 4**, examples from Ref [17], Table 7, of large errors due to inappropriate comparisons are presented. As can be observed from **Table 3**, the appropriate comparison of geometry-based strains results in errors within the MD

https://doi.org/10.52202/078572-0045

5-2 reported scatter band. In contrast, the errors reported in **Table 4** are large due to inappropriate comparison of geometry-based strains with equivalent plastic strains for unrestrained dents at pressure.

Table 3. Comparisons of curvature-based strains with FE effective strains (excerpt from Table 7 of Ref [17])

	At Pressure		At Indentation		At Indentation	
Low OD/WT, OD4.5", Indenter-7" Transverse Bar	FE Effective Strain	5.9	FE Effective Strain	7.53	ASME effective strain from FE profiles	7.53
	ASME effective strain	4.86	Predicted ASME effective strain (Eq 3)	7.05	Predicted ASME effective strain (Eq 3)	9.83
	%Error	−17.64	%Error	−6.49	%Error	30.52
High OD/WT, OD24", Indenter -14" Hemispherical	FE Effective Strain	5.41	FE Effective Strain	8.66	ASME effective strain from FE profiles	8.66
	ASME effective strain	4.78	Predicted ASME effective strain (Eq 3)	8.91	Predicted ASME effective strain (Eq 3)	9.77
	%Error	−11.61	%Error	2.83	%Error	12.74

Table 4. Comparison of curvature-based strains with FE equivalent plastic strain for re-rounded unrestrained dents (excerpt from Table 7 of Ref [17])

Low OD/WT, OD4.5", Indenter-7" Transverse Bar				High OD/WT, OD24", Indenter -14" Hemispherical			
After Re-rounding		After Re-rounding		After Re-rounding		After Re-rounding	
FE Equivalent Plastic Strain	12.3	FE Equivalent Plastic Strain	12.3	FE Equivalent Plastic Strain	8.7	FE Equivalent Plastic Strain	7.3
FE "Effective" Strain	5.9	Modified ASME effective strain	4.85	FE "Effective" Strain	5.41	Modified ASME effective strain	4.85
%Error	−52.03	%Error	−60.57	%Error	−37.79	%Error	−33.56

In Ref [18], additional analyses were performed where the Equation 3 predicted indentation ASME effective strains were inappropriately compared against FE equivalent plastic strains at indentation. As discussed earlier, Equation 3 does not distinguish between OD and ID strains and only deals with the maximum of these two values. In Ref [18], Equation 3 predictions have been inappropriately compared against both OD and ID equivalent plastic strains (**Figure 21**), which can result in large errors. Furthermore, the dent maximum equivalent plastic strain values being compared in Ref [18] are not always from the dent peak. This further invalidates these comparisons as the Equation 3 predictions are always located at the dent peak.

https://doi.org/10.52202/078572-0045

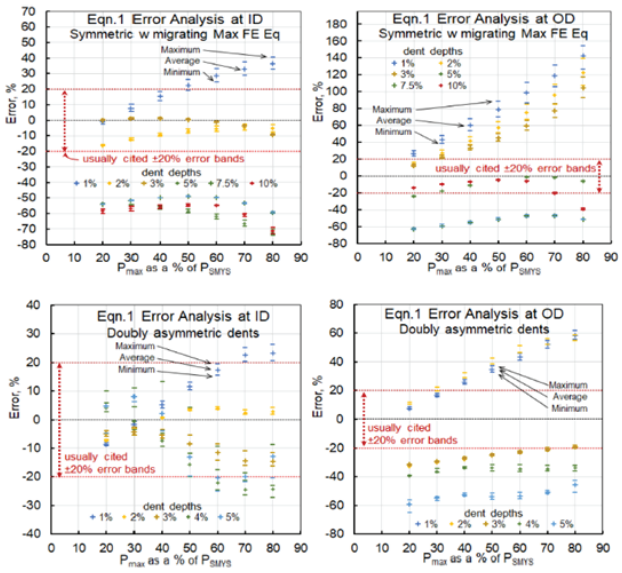

Figure 21. %Errors between Equation 3 predictions and migrating FE equivalent plastic strains [18]

Mesh refinement

As discussed in the dent fatigue life section, the FE modelling framework employed in the PRCI/CEPA projects has been extensively validated against full-scale results. This validated FE modelling framework was employed in the MD 5-2 project for comparative analysis, where ASME and FE effective strains were compared. In Ref [18], Section 3.1, a FE mesh sensitivity study on a dent (8.625"OD, 0.332"WT, X52 grade, 7" Spherical indenter, 0.6%OD indentation depth) was performed comparing equivalent plastic strain values across a range of mesh sizes (0.25 to 4 mm) (**Figure 22**). It was demonstrated that the maximum equivalent plastic strain values converged at or below 0.5 mm mesh size and did not converge at the mesh size (2 mm for 8" OD pipe) employed in the PRCI/CEPA projects. It must be noted that, the focus in the MD 5-2 research project was on geometry-based strains and comparison against equivalent plastic strains is not relevant with regards to this when considering the ASME approach.

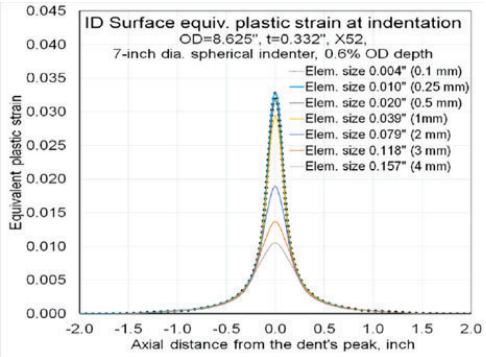

Figure 22. Mesh sensitivity study conducted in Ref [18]

https://doi.org/10.52202/078572-0045

Mesh sensitivity studies were also conducted in the present paper and the results are discussed below. The same scenario used in the mesh sensitivity study in Ref [18], was recreated using the FE modelling approach employed in PRCI/CEPA for two different mesh sizes - 0.5 mm and 2 mm. Two additional scenarios, one with dent on stiff pipe (6.625"OD, 0.281"WT, X52, 5" Spherical Indenter, 3%OD Indentation Depth) and the other with dent on a compliant pipe (24"OD, 0.34"WT, X52, 25.5" Spherical Indenter, 3%OD Indentation Depth) were also considered. In both scenarios, a very fine (0.4 mm and 0.8 mm) and a coarse mesh (both 4 mm) were applied. The coarse mesh size adopted is representative of the mesh sizes employed in the PRCI/CEPA projects. Both additional scenarios, represent more severe indentations compared to the Ref [18] scenario and should represent a greater modelling challenge.

Since, the primary focus of the MD 5-2 project was geometry-based strains, the indentation dent peak ASME effective strains evaluated from the FE profiles, across the different mesh sizes have been compared in **Table 5**, for the three scenarios. As can be observed, very small differences exist between the fine and coarse mesh sizes, which support the adequacy of the mesh sizes adopted in the PRCI/CEPA projects in predicting geometry-based strains.

Table 5. Comparison of curvature-based strains evaluated from FE profiles

	Finer Mesh		Coarser Mesh		
Dent	Mesh Size	ASME effective strain	Mesh Size	ASME effective strain	%Error
8.625"/0.332", 7" Spherical, 0.6%OD	0.5 mm	4.3%	2 mm	4.3%	0.25%
6.625"/0.281", 5" Spherical, 3%OD	0.4 mm	21%	4 mm	20.0%	4.6%
24"/0.34", 25.5" Spherical, 3%OD	0.8 mm	6.4%	4 mm	6.3%	1.6%

The equivalent plastic strain values were also compared across the different mesh sizes, for three scenarios. The axial distributions of equivalent plastic strain after indentation, extracted from the nodes along the dent center line, on the pipe ID surface, have been presented in **Figure 23**, for the three scenarios studied here. It can be observed that for all three scenarios good agreement exists between the fine and coarse mesh cases. For the scenario recreated from Ref [18] (**Figure 23**a), only a 5% difference exists between the maximum equivalent plastic strain values, while an almost 40% difference was reported between the 0.5 mm and 2 mm mesh sizes in Ref [18]. The large differences in strain values between the mesh sizes reported in Ref [18], may be due to the extraction of elemental strain values (from element centroid or integration points) [33] rather than nodal values, along a line passing through the dent peak. Commercial FE software offer both elemental and nodal results. If strain values are extracted from the interior of the element (e.g., element centroid), across different mesh sizes, then the location of extraction do not coincide for the different element sizes. The discrepancy in location of extraction can result in larger differences in the extracted strain values, as shown in **Figure 24** for the scenario recreated from Ref [18]. In **Figure 24**, it can be observed that a

https://doi.org/10.52202/078572-0045

larger difference (20%) in maximum equivalent plastic strain exists between the two mesh sizes, similar to the observations in Ref [18]. No specifics have been provided in Ref [18] with regards to the location of extraction of strain values.

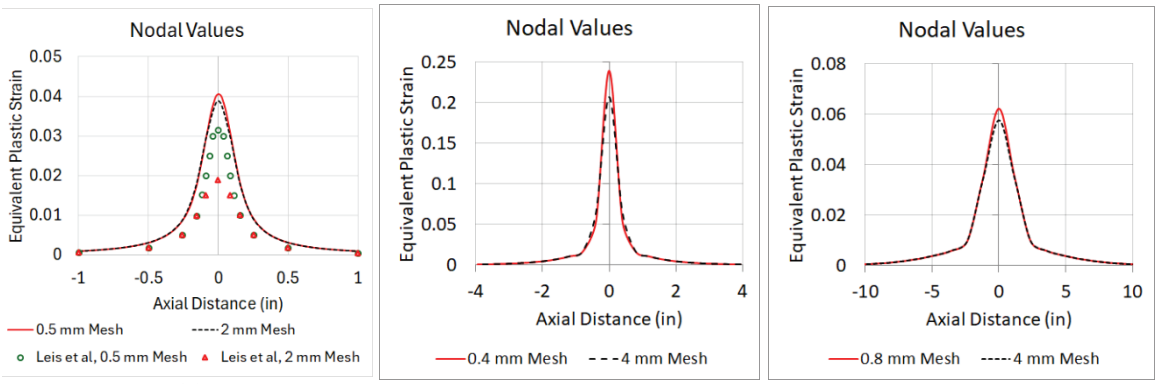

(a) (b) (c)

Figure 23. Axial distribution of equivalent plastic strains for dents in (a) 8"OD (b) 6.625" OD (c) 24" OD pipes, across different mesh sizes

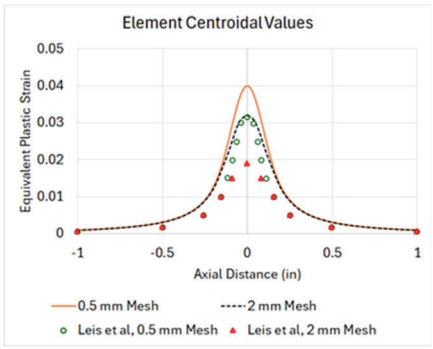

Figure 24. Discrepancy in equivalent plastic strain values from two mesh sizes, due to extraction from element centroids

Kinked dents

In Ref [17], discussions have been presented regarding the EPRG and API 579 recommendations for "kinked" dents (bending strain > 10% or dent radius of curvature < 5*WT). It is recommended that shell elements are not suitable for such cases and solid elements be used instead. About 5% of the FE dents employed in the PRCI/CEPA projects exhibited bending strains >10%. As part of the present study, a full-scale test and a series of numerical simulations were conducted to evaluate the accuracy of shell elements in modelling a very sharp kinked dent. A kinked dent was fabricated on a 32" OD pipe using a 1.5" diameter indenter, with a 14% OD indentation depth. A maximum dent peak bending strain of approximately 20% was achieved, which is well above the kinked dent threshold. A digital image correlation (DIC) system was used to track the dent strains during indentation (**Figure 25**). The DIC system employs high resolution cameras to measure the surface strain in the full-scale indentation test. FE simulations of the indentation test were conducted using both solid and shell elements – both used 1 mm elements in the contact area. Both solid and shell element models agreed well with the maximum principal strain field measured by the DIC setup

https://doi.org/10.52202/078572-0045

(**Figure 26**). Only a 12% difference in the reported strains (e.g., 34% versus 30% strain) was observed between the maximum principal strain values from DIC and shell model (3% difference between DIC measurement and solid model). Equivalent plastic strains were also evaluated for the solid and shell models and the values agreed well (**Figure 27**). A coarser shell mesh (3 mm) was also tested, and it exhibited a maximum equivalent plastic strain value only 8% lower than the solid model. These results demonstrate that the implemented shell models were able to accurately predict the strains at indentation. In the dent fatigue discussion section of this paper, good agreement was also observed between FE (shell) predicted and experimental strain ranges for several kinked dents. These results demonstrate that the generalized statement about the applicability of shell models made in Ref [17] may not be accurate.

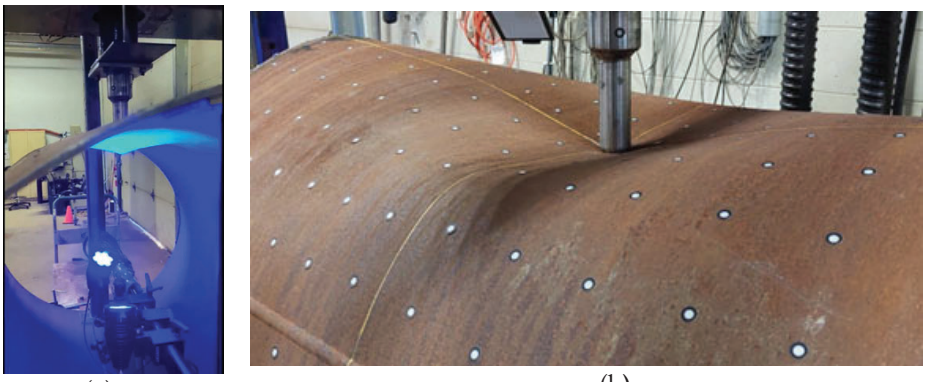

(a) (b)

Figure 25. Kink dent full-scale test photos. (a) DIC setup (b) Pipe indentation

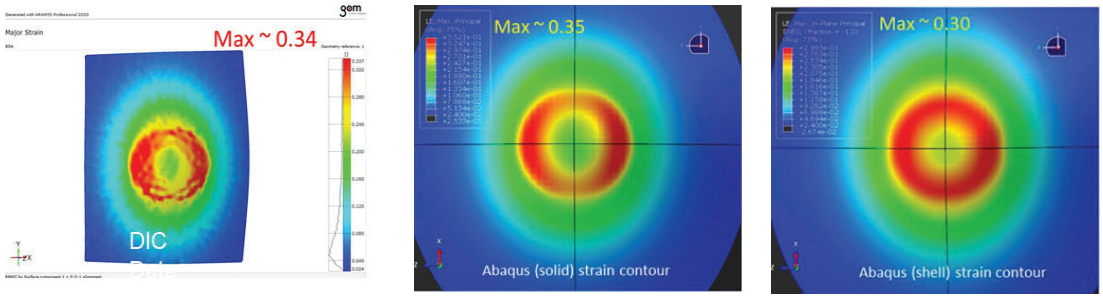

(a) (b) (c)

Figure 26. Maximum principal strain contours from (a) DIC (b) solid model (c) shell model

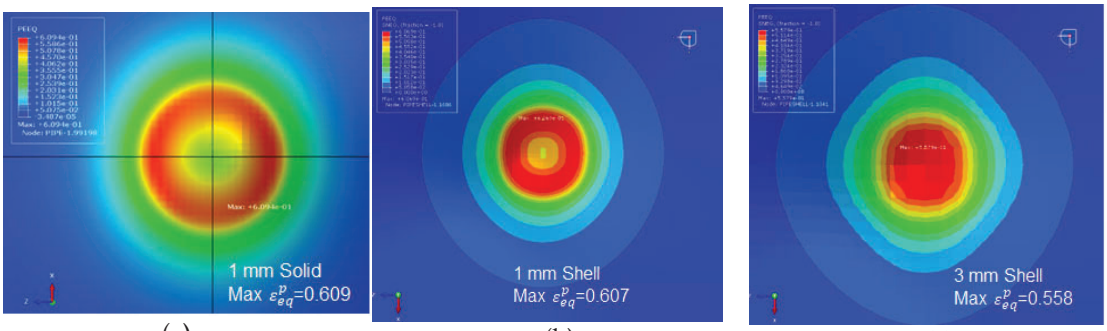

(a) (b) (c)

https://doi.org/10.52202/078572-0045

Figure 27. Equivalent plastic strain contours from (a) 1 mm solid (b) 1 mm shell and (c) 3 mm shell models

Comparisons against exceptional cases

Regression models like Equation 3 developed in the MD 5-2 project, were developed to address practical scenarios which can be reliably measured in the field. Equation 3 was fitted using a large dataset (24,000 FE cases) that consist of such scenarios. Equation 3 is not a mechanistic model, and its predictive accuracy decreases if applied to cases that are significantly outside the domain of fitting. In Ref [17] and [18], several of the comparative analyses presented are with regards to exceptional cases that are significantly outside the domain of fitting of Equation 3, which result in very large errors. Furthermore, several of these cases were below the detection threshold of current ILI technologies and therefore cannot be reliably measured in the field.

Application of Equation 3 to very shallow dents

In Section 3.4.5 of Ref [18], the predictive accuracy of Equation 3 was tested against FE data from a wide range of dent depths. Equation 3 was applied across the different dent depths and the predicted indentation ASME effective strains were inappropriately compared to equivalent plastic strains at indentation. The resulting errors across the dent depths have been provided in **Figure 28**. Of interest, there are two dent depth cases (highlighted in **Figure 28**) which exhibit very large Equation 3 prediction errors, ranging from 25% to 150%, while the rest of the dent depths exhibit errors within ±20%. The two problematic cases were recreated in the present study, using the PRCI/CEPA FE modelling template. The unrestrained dent depths of these cases, under pressure, are 0.15 mm (0.07% OD) and 0.3 mm (0.1% OD). Based on the dent depths, it can be stated that these cases are well below the specified performance threshold of detection of ILI tools and would not be credibly detected or be included in real world integrity management programs.

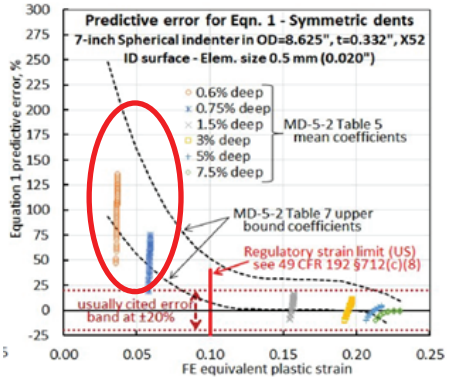

Figure 28. %Errors of Equation 3 predicted indentation strains against equivalent plastic strains at indentation, across multiple indentation depths [18]

Micro-strain inputs into Equation 3

In Section 3.4.2 (1) of Ref [17], investigations were conducted on the applicability of Equation 3 in scenarios involving re-rounded strain values approaching zero ($E_P \rightarrow 0$). Strain values as small as

10^{-6} were considered. Modelling such micro-strain cases have no practical value as they do not represent any threat to pipeline integrity.

Dent formed using complex indenter

In Section 3.4.2 (3) of Ref [17], the predictive performance of Equation 3 has been compared against FE results of a dent formed using a complex-shaped indenter topped with a 0.6" radius dimple. Due to the sharpness of the dimple, the ASME effective strain at indentation was very high (approximately 50%). Equation 3 was fit using a dataset where the highest ASME indentation strain value was about 40%, with <1% of dent cases having strains greater than 30% (Table 1). Considering these factors, it can be stated that this dent case represents a significant outlier. The Equation 3 output underpredicted the indentation strain by almost 25%. Despite this case being an outlier, the prediction error is still within the observed scatter of Equation 3.

Summary of strain discussions

In the preceding sections, the major concerns raised in Ref [17], [18] and [19], regarding the strain work presented in MD 5-2 have been addressed. It is noted that:

- The investigations conducted in the present study revealed that the large errors demonstrated in Ref [17], [18], and [19] are largely due to comparisons outside the scope of the MD 5-2 strain work. For example, the majority of the comparisons of the MD 5-2 curvature-based effective strains are made against accumulated equivalent plastic strains, which result in large errors, due to the inherent differences between these two quantities.
- Several example cases explored have been exceptional cases which can be difficult to detect and sized reliably by current ILI technologies.
- In the examples presented in this study, and in Ref [17], [18] and [19] , if the comparisons of the MD 5-2 strain formulations are limited within the intended scope of the MD 5-2 work (comparison against curvature/geometry-based strains), then the errors were found to be within the expected scatter.
- Mesh sensitivity studies were also presented to support the validity of the FE modelling template used in the MD 5-2 project, within the intended scope of the work.

The results of this study show that, except for significant outliers, the MD 5-2 strain models should work as intended for most practical scenarios encountered in the field.

Concluding Remarks

A significant amount of work has been performed under the various PRCI/US DOT [1] [2] [3] [4] [5] [6] [10] [12] [14] [15] [16] and CEPA [7] [8] [9] projects to further the understanding of the impact of mechanical damage in pipeline integrity management. These projects included extensive full-scale testing of dents, comprehensive finite element modelling of dents, development of engineering tools for dent integrity screening and assessment, extensive validation of the integrity management tools against experimental and field data and quantification of the effect of ILI measurement variation in

https://doi.org/10.52202/078572-0045

dent integrity assessment. The major takeaways from the discussions provided in this paper are as follows:

- Extensive dent full-scale testing (127) has been performed across different pipe geometries, dent shapes, cyclic pressure loading and restraint conditions. 20% of the tests were on dents removed from the field. The full-scale test data were used to validate the finite element models that were employed to develop the various dent engineering assessment tools, thereby confirming the adequacy of the mesh size used in these models
- The dent fatigue life assessment engineering tools have been extensively validated against the full-scale test experimental fatigue data, comparison of stress ranges predicted using Level 2 with FE analysis of 1000 in-service dents and operator provided in-ditch inspection data on more than 1000 field dents. The field dent data provided by the operators were for dents that had been remediated based on their integrity management programs. It was demonstrated that even with a conservative use of the dent fatigue assessment tools, remediation could have been safely avoided for more than 60% of the dents considered. The assessments correctly identified all dents that had developed leaks and most of the dents with cracks with low remaining fatigue life
- The ILI dent measurement variation was quantified using extensive data from pull trials where nine ILI service providers participated in running their ILI tools, multiple times, through pipe test strings with more than 100 dents. The effect of the measurement variation on dent fatigue life, restraint parameter, and strain predictions was quantified. Dent parameters were consistently extracted by the participating service providers, confirming that the shape parameter-based approach is reproducible by third parties when used on ILI data
- The issues raised in recent publications regarding the work completed in the PRCI/CEPA projects were addressed. The majority of the issues raised stemmed from misinterpretation of API RP 1183 or misapplication of the engineering tools outside the scope of development of these tools, some with cases which cannot be reliably measured in the field or with scenarios that would not pose any integrity threat. Application within the scope of the models resulted in predictions within the expected scatter

The extensive body of research and validation work lends confidence in the PRCI/CEPA developed assessment tools which provide reasonable and conservative dent fatigue life and strain predictions. The objective of developing these tools was to provide simple, engineering solutions to complex integrity problems. As demonstrated by the validation studies, these tools exhibit good predictive accuracy for a wide variety of cases but may not be applicable to all conceivable scenarios which may include significant outliers. It is important to consider whether such outlying scenarios are realistic or practical. It is also important to consider if such cases can be reliably measured by available tools. If not, any analysis approach, even highly involved FEA tools, will be subject to the measurement errors and will not result in reliable predictions.

https://doi.org/10.52202/078572-0045

The PRCI/CEPA tools have been presented as part of API RP 1183 first edition. Opportunities for improvement in the first edition, having been in use for approximately 4 years, have been identified beyond those discussed in this paper and are being addressed in the preparation of a second edition.

References

[1] S. Tiku, V. Semiga, A. Dinovitzer and B. John, "Full Scale Fatigue Testing of Dents (Plain Dents and Dents Interacting with Welds and Metal Loss) MD4-2," PRCI Catalog No. PR-214-073510-R01, 2018.

[2] S. Tiku, A. Eshragi, B. John and A. Dinovitzer, "Full Scale Testing of Interactive Features for Improved Models," MD 4-11 US DOT PHMSA DTPH56-14-H-00002, 2017.

[3] S. Tiku, A. Eshragi, B. John and A. Dinovitzer, "Full Scale Testing of Shallow Dents with and without Interacting Features MD4-14," PRCI Catalog No. PR-214-163714, 2019.

[4] S. Tiku, B. John, B. Shiari and A. Rana, "Full-Scale Testing of Field Dents," PRCI PR-214-183816, 2021.

[5] S. Tiku, A. Eshragi, A. Rana and A. Dinovitzer, "Fatigue Life Assessment of Dents with and without Interacting Features MD4-9," PRCI Catalog No. PR-214-114500-R01.

[6] S. Tiku, A. Rana, B. John, A. Roostaei and A. Dinovitzer, "Improvement in Dent Assessment and Management Tools," PRCI PR-214-223810, 2023.

[7] A. Eshragi, S. Tiku, B. John and M. Ghovanlou, "Management of Shallow Restrained Dents," CEPA, 2018.

[8] A. Eshragi, S. Tiku and A. Rana, "Management of Unrestrained Dents," CEPA, 2019.

[9] A. Rana, S. Tiku and V. Semiga, "Management of Dents," CEPA, CSA SPE-225.4:22, 2021.

[10] A. Rana and S. Tiku, "Guidance for Performing an Engineering Critical Assessment for Dents on Natural Gas Pipelines," MD 5-03 PRCI Catalog No. PR-214-223806, 2023.

[11] American Petroleum Institute, "API RP 1183, Assessment and Management of Dents in Pipelines, First Edition," API, 2020.

[12] S. Tiku, A. Rana and B. John, "Evaluation of API RP 1183 Dent Fatigue Life Analysis Approach using In-Service Dents Data, MD-2-5," PRCI PR-214-213800, 2024.

[13] S. Tiku, A. Rana, B. John, A. Dinovitzer and M. Piazza, "Validation of dent fatigue life screening and assessment methods in API RP 1183," *International Pipeline Conference,* 2024.

[14] A. Rana, S. Tiku and A. Dinovitzer, "Improve Dent/Cracking Assessment Methods," PRCI Catalog No. PR-214-203806-R01 , 2022.

[15] S. Tiku, A. Rana, B. John and A. Dinovitzer, "Performance Evaluation of ILI Systems for Detecting and Discerning Metal Loss, Cracks and Gouges in Geometric Anomalies," PRCI Catalog No. PR-214-203820, 2023.

[16] S. Tiku, A. Rana, B. John and A. Dinovitzer, "Performance Evaluation of ILI Systems for Dents and Coincident Features," US DOT, 2024, 2024.

[17] B. N. Leis, M. A. Eshragi, B. A. Dew and Y. F. Cheng, "Dent strain and stress analyses and implications concerning API RP 1183 - Part I: Background for dent geometry and strain analyses during contact and re-rounding," *Journal of Pipeline Science & Engineering,* 2023.

https://doi.org/10.52202/078572-0045

[18] B. N. Leis, M. A. Eshragi, B. A. Dew and Y. F. Cheng, "Dent strain and stress analyses and implications concerning API RP 1183 - Part II: Examples of dent geometry and strain analyses during contact and re-rounding," *Journal of Pipeline Science and Engineering,* 2023.

[19] B. N. Leis and M. A. Eshragi, "Commentary on API RP 1183 – Dent Assessment and Management," *Pipeline Pigging and Integrity Management Conference,* 2024.

[20] S. Polasik, S. Wu, J. Bratton, R. Dotson and R. Sager, "The State Of Dent Screening And Shape-Based Assessments," *14th International Pipeline Conference,* 2022.

[21] X.-K. Zhu, "A verification study of fatigue-based methods in API RP 1183 for estimating fatigue life of pipeline dents," *International Journal of Pressure Vessels and Piping,* vol. 205, 2023.

[22] "API 579/ASME FFS-1 June 5, 2007, The American Society of Mechanical Engineers and the American Petroleum Institute.".

[23] A. Rana, S. Tiku, M. Piazza and T. Burns, "Enhancement of mechanical damage crack evaluation," *International Pipeline Conference,* 2022.

[24] American Society of Mechanical Engineers, "ASME B31.8-2018, Gas Transmission and Distribution Piping System," ASME, 2018.

[25] A. Rana, S. Tiku, A. Dinovitzer, M. Piazza and M. Tomar, "Modification of dent-weld interaction factors and dent corrosion-gouge discrimination methodology incorporated in API RP 1183," *International Pipeline Conference,* 2024.

[26] "British Standards Institute, Guide to Methods for Assessing the Susceptibility of Flaws in Metallic Structures," BS7910:2005, 2013.

[27] E. Neto, D. Peric and D. Owen, Computational Methods For Plasticity: Theory And Applications, John Wiley & Sons, Ltd, 2008.

[28] J. Lemaitre and J. L. Chaboche, Mechanics of solid materials, Cambridge University Press, 2002.

[29] R. W. Revie, Oil and Gas Pipelines: Integrity and Safety Handbook, John Wiley & Sons, 2015.

[30] T. Hang, G. Zheng, J. Sun, D. Kohlenberg and M. Di Blasi, "Improvements to B31.8 Dent Strain Estimation and Assessment of Dent Formation Induced Cracking," *15th International Pipeline Conference,* 2024.

[31] M. J. Rosenfeld, P. C. Porter and J. A. Cox, "Strain Estimation Using Vecto Deformation Tool Data," *ASME 2nd International Pipeline Conference,* 1998.

[32] C. Okoloekwe, M. Kainat, D. Langer, S. Hassanien, J. R. Cheng and S. Adeeb, "Three-Dimensional Strain-Based Model for the Severity Characterization of Dented Pipelines," *Journal of Nondestructive Evaluation, Diagnostics and Prognostics of Engineering Systems,* vol. 1, no. 3, 2018.

[33] Dassault Systemes, ABAQUS User's Manual, 2022.

https://doi.org/10.52202/078572-0045